

## Supporting Information

### Long-Term Stability of Oxide Nanowire Sensors via Heavily-Doped Oxide Contact

Hao Zeng,<sup>†</sup> Tsunaki Takahashi,<sup>\*,†</sup> Masaki Kanai,<sup>†</sup> Guozhu Zhang,<sup>†</sup> Yong He,<sup>‡</sup> Kazuki Nagashima<sup>†</sup> and Takeshi Yanagida<sup>\*,†</sup>

<sup>†</sup>*Institute for Materials Chemistry and Engineering, Kyushu University, 6-1 Kasuga-Koen, Kasuga, Fukuoka 816-8580, Japan*

<sup>‡</sup>*Key Laboratory of Optoelectronic Technology and Systems of the Education Ministry of China, Chongqing University, Chongqing 400044, P. R. China*

#### Contents

- **Annealing Effects on Resistivity and Morphology of ATO Film**
- **Extraction of Contact Resistance ( $R_c$ )**
- **Current Degradation of Ti Contact SnO<sub>2</sub> Nanowire Devices under Heating**
- **Extraction of Sensor Response**
- **Thermal Decomposition of PEN Substrate**

## Annealing Effects on Resistivity and Morphology of ATO Film

Sb-doped SnO<sub>2</sub> (ATO) contact layer was deposited at room temperature. The  $I$ - $V$  characteristics of ATO contact devices indicate that the contact resistance ( $R_c$ ) of ATO contact is considerably high without annealing (Fig. 2b). Figure S1 shows the thermal annealing effects on the morphology and resistivity of an ATO thin film. As the annealing temperature increases, the ATO film resistivity greatly reduces. One of the possible origins of the huge decrease in the resistivity is the improvement of the crystallinity of ATO films by annealing. The obtained annealing temperature dependence of resistivity (Fig. S1b) agrees well with the growth temperature dependences of ATO film resistivity reported by Kim *et al.*<sup>1</sup> Kim *et al.* have reported that a SnO<sub>2</sub>:Sb film changes from amorphous to polycrystalline structure over 200 °C and its grain size increases as temperature increases up to 600 °C.<sup>1</sup> Kim *et al.* also have given an explanation that the decrease in the resistivity is due to the polycrystallization and increase in the grain size, which suppress the grain boundary scattering of carriers. The morphological changes of our sample by annealing (Fig. S1a) seems to be consistent with their explanation: the grain size increases as temperature increases.

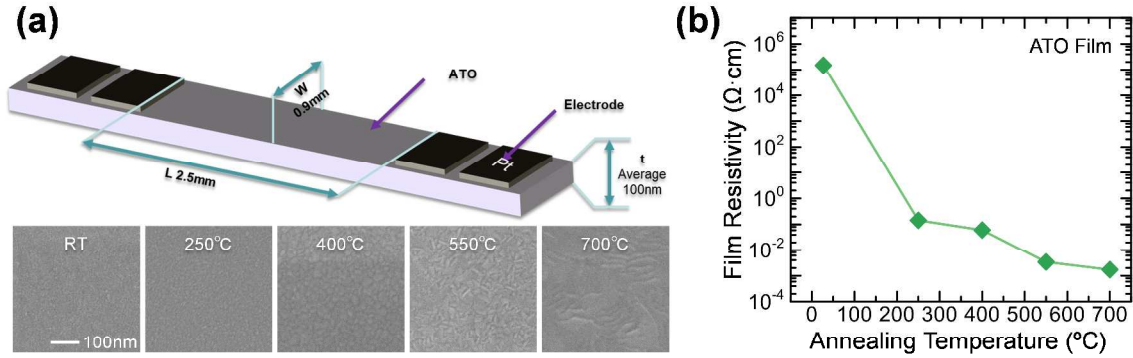


**Figure S1.** (a) Schematic image of an Sb-doped SnO<sub>2</sub> (ATO) thin film device and FESEM images of ATO film after annealing at various temperatures (10 min, 10 Pa Ar). “RT” indicates the FESEM image of ATO film without annealing. (b) Relationship between ATO film resistivity and annealing temperature. The resistivity was extracted by four-probe technique.

## Extraction of Contact Resistance ( $R_c$ )

$R_c$  is extracted as  $R_c = R_{2p} - R_{4p}$ , where  $R_{2p}$  and  $R_{4p}$  are resistances which are measured using four-terminal devices by two- and four-probe techniques, respectively. For  $R_{2p}$ , the voltage bias from  $-1$  to  $+1$  V was applied between the inner two terminals. For  $R_{4p}$ , the voltage bias from  $-2$  to  $+2$  V was applied between the outer two terminals and the voltage difference between the inner two terminals was measured. Since  $I$ - $V$  characteristics show non-linear curve with a Schottky diode like contact, a resistance extraction from a linear fitting might cause an error due to the non-linearity. To avoid the error,  $R_{2p}$  and  $R_{4p}$  were evaluated from the slope of  $I$ - $V$  curve near  $V=0$  region by fitting the  $I$ - $V$  characteristics with a 6-order function, namely

$$I(V) = k_0 + k_1V + k_2V^2 + \dots + k_6V^6,$$

$$R = \left( \frac{dI}{dV} \Big|_{V=0} \right)^{-1} = \frac{1}{k_1}.$$

## Current Degradation of Ti Contact SnO<sub>2</sub> Nanowire Devices under Heating

As shown in Fig. S2, the current of Ti contact devices was gradually reduces as heating time increases. The  $I$ - $V$  curve of Ti contact shows a Schottky diode like characteristics at an intermediate state between the initial and long-term operation condition (2008 hours). The transition behavior from Ohmic to Schottky characteristics indicates that the Ti contact layer was gradually oxidized and the Schottky barrier height/thickness were gradually increased with the oxidation.

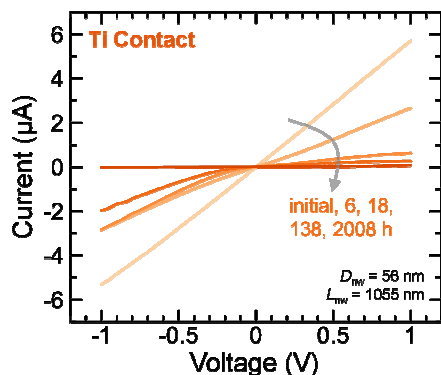


**Figure S2.**  $I$ - $V$  characteristics of a Ti contact SnO<sub>2</sub> nanowire device measured by two-probe technique.  $I$ - $V$  characteristics as fabricated (initial) and after heating at 200°C in open air (6, 18, 138 and 2008 hours) are shown.

## Extraction of Sensor Response

The sensor response was evaluated as  $R/R_0 \times 100\%$ , where  $R$  and  $R_0$  are the nanowire resistance and that under N<sub>2</sub>/dark condition, respectively. For Ti contact sensor devices under a long-time heating, the high  $R_c$  causes a considerable error in the  $R/R_0$  as shown in Figs. 4a,d. Therefore,  $R_0$  in Fig. 4 and  $R$  used in Figs. 4c,f were extracted as time-averaged resistances with and without NO<sub>2</sub>/UV as shown in Fig. S3.

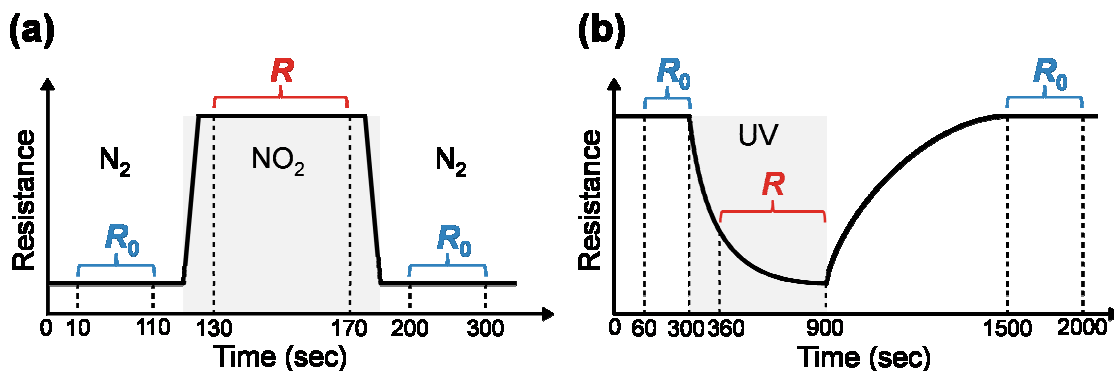


**Figure S3.** Schematics of sensor response characteristics of (a) NO<sub>2</sub> and (b) photo (UV light) detection. Averaging time periods for the sensor response calculation ( $R/R_0 \times 100\%$ ) are indicated.

## Thermal Decomposition of PEN Substrate

As shown in Fig. 5d, the  $R_c$  of Ti contact devices on PEN substrates was lower than that on Si substrates (Fig. 2d). The low  $R_c$  of devices on the PEN substrate is probably due to the thermal decomposition of PEN substrates. Generally, a polyester such as PEN and polyethylene terephthalate (PET) partially decomposes to the several kinds of organic molecules (eg. fatty acids) at a high temperature due to the instability of ester bonding.<sup>2,3</sup> The decomposed molecules might passivate the surface of electrodes and suppress the oxidation of the Ti contact layer.

## References

1. Kim, H.; Piqué, A., Transparent conducting Sb-doped SnO<sub>2</sub> thin films grown by pulsed-laser deposition. *Appl. Phys. Lett.* **2004**, *84*, 218-220.
2. Girija, B. G.; Sailaja, R. R. N.; Madras, G., Thermal degradation and mechanical properties of PET blends. *Polym. Degrad. Stab.* **2005**, *90*, 147-153.
3. Holland, B. J.; Hay, J. N., The thermal degradation of PET and analogous polyesters measured by thermal analysis–Fourier transform infrared spectroscopy. *Polymer* **2002**, *43*, 1835-1847.